BENDING FATIGUE PROPERTIES OF NANOHONEYCOMB BEAM STRUCTURES

Ji Hoon Jeon*, Pyung Soo Lee, Kun-Hong Lee**,**
Hyun Chul Park*, and Woonbong Hwang*
***Dept. of Mechanical Engineering, Pohang University of Science and Technology (POSTECH), Pohang, Republic of Korea.**
****Dept. of Chemical Engineering, Pohang University of Science and Technology (POSTECH), Pohang, Republic of Korea.**

Keywords: *AAO, Nanohoneycomb, Bending Fatigue, Nano-UTM*

Abstract

Nanohoneycomb structures of Anodic Aluminum Oxide (AAO) were fabricated by a two-step anodization process. Nanohoneycomb cell structures can widely used in a variety of engineering applications, in view of their large surface area and controllable surface properties. For stable mechanical structures of nanohoneycomb structures, fatigue properties are very important. The bending fatigue properties of nanohoneycomb structures were measured using a Nano-Universal Testing Machine (UTM) under cyclic three-point bending. The mean values of the experimental results were compared with several single load level fatigue life prediction equations with good agreement, although there were large deviations of experimental fatigue life data among samples with the same load level. The present results can be used as a design guideline in applications of nanohoneycomb structures.

1 Introduction

Conventional sandwich structures including honeycomb structures are widely used in a variety of engineering applications, in view of their high strength-to-weight ratio and flexural rigidity-to-weight ratio. With the rapid development of nanotechnology, honeycomb cell structures of nano/micrometer scale have now been fabricated using various methods[1-3]. Honeycomb structures with nanometer size pores are known as nanohoneycomb structures. Anodic aluminum oxide (AAO) films, which are fabricated by the anodization of aluminum, make favorable nanohoneycomb structures because of the simplicity of the fabrication process, the high aspect ratio, the self-ordered hexagonal pore structure, and the ease of control of the pore dimensions[3]. AAO films can be used more widely than conventional honeycomb structures, finding application in various fields. The mechanical properties of nanohoneycomb structures are of prime importance in creating stable products. To fabricate stable mechanical structures using nanohoneycomb structures, not only static properties but also fatigue properties are very important. This study investigates the bending fatigue properties of nanohoneycomb structures measured using a Nano-Universal Testing Machine (Nano-UTM) under cyclic three-point bending.

2 Fabrication

Details of the nanohoneycomb fabrication process are as follows:

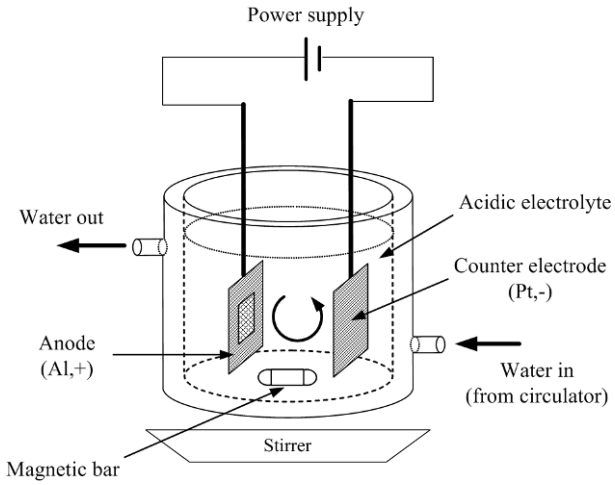

Fig. 1. Schematic diagram of fabrication equipment

(a) The specimen was first electro-polished. A pure Al sheet (99.999 %), 1 mm thick, was degreased in acetone by ultrasonication. The specimen was then rinsed several times in ethanol for at least

15 minutes and finally rinsed in deionized water. Next, the specimen was electro-polished in a mixture of perchloric acid and ethanol ($HClO_4$: C_2H_5OH = 1:4 volumetric ratio) to remove surface irregularities. The specimen was then used as an anode, with a flat Pt or curved Al sheet as a cathode. A potential difference of DC 20 V was applied between the cathode and the anode for 60 to 90 seconds, and the solution temperature was maintained at 7℃ during electro-polishing. The schematic diagram is shown in Fig. 1.

(b) Next, the first anodization of the specimen was performed. The specimen was rinsed several times in ethanol for more than 15 minutes, then rinsed in deionized water, and finally dried in an air stream. The anodization step was then carried out in 0.3 M oxalic acid solution. This anodization was performed for more than 8 hours. The experimental setup was the same as that used in electro-polishing, except that oxalic acid was used instead of the perchloric acid-ethanol solution.

(c) The AAO layer was removed by immersing the specimen in a mixture of 1.8 wt% chromic acid and 6 wt% phosphoric acid at 65℃ for 5 hours.

(d) An initial AAO film was obtained by a second anodization with oxalic acid under the same conditions as the first. The thickness of the specimen was determined by the duration of the second anodization.

(e) The pores were widened and the barrier layers were thinned by etching in 0.1 M phosphoric acid solution at 30℃. The duration of etching was chosen according to the desired pore diameter.

At every step, the solution was stirred at constant speed with a magnetic stirring bar. The electro-polishing and the anodization were all carried out in a jacketed beaker in a refrigerated circulating bath so as to maintain the temperature of the solution constant. The surface morphology of the fabricated structures was tailored to a beam shape. Details of the fabrication next process are as follows

(f) On the previous AAO nanohoneycomb structure, a thin aluminum layer was deposited by thermal evaporation. This step generates a surface with high reflectivity, needed for lithography of the nanohoneycomb patterns.

(g) The pattern was transferred to the underlying aluminum layer (the transfer layer) by immersing the sample in an etchant. The exposed area was removed by the aluminum etchant, whereas the protected area covered by PR remained unetched.

(h) The microstructure was generated on the AAO substrate by etching the sample. The part of the AAO substrate that was exposed to the etchant was removed, whereas the pattern protected by the aluminum transfer layer remained unetched. Finally, mercury chloride solution was used to separate the alumina and the aluminum, to obtain the patterned microstructure. The final product is shown in Fig. 2.

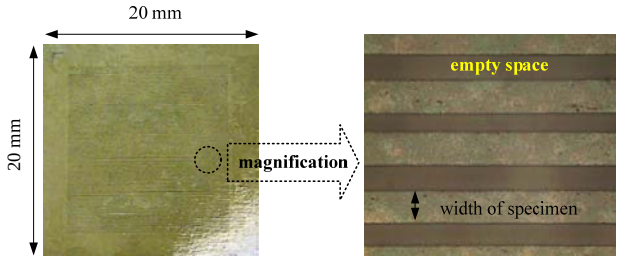

Fig. 2. Nanohoneycomb specimens

3 Geometry

The nanohoneycomb structure consists of open, porous, and clogged layers as is shown Fig. 3.

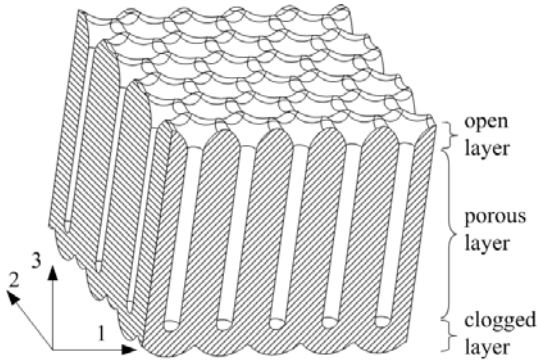

Fig. 3. Layers of nanohoneycomb structures

The ratios of the height of the open and clogged layers to the total height are very small. For example, the thickness of the tensile specimen for Nano-UTM was 57 μm, and the thicknesses of the open, porous, and clogged layers were respectively 0.0404 μm, 56.8 μm and 0.064 μm. The heights of the open and clogged layers are negligible. The interpore distance was 90-110 nm, and the pore diameter was 25-35 nm. The pores were uniformly distributed, as in conventional honeycomb structures; as a result the

nanohoneycomb is an orthotropic material within the grain boundary layer.

4 Fatigue Life Models

Some Single Load Level Fatigue Life Prediction Equations (SFLPE) were compared with the fatigue test results, as follows [4, 5]:

Hwang's Equation: $N = [M(p^B - q^B)]^{1/C}$ (1)

Basquin's Relation: $N = (q/p)^{-1/A}$ (2)

S-N Curve: $q = k \log N + d$ (3)

where N is the fatigue life and q is the applied load level to the static fatigue load. M, B, A, k, p and d are material constants.

The static failure occurs at one quarter cycle which could be considered as n is 0 or 1. This point is represented as (1,0) or (1,1) in q-N plane regardless of materials. The above equations do not pass one fixed point at static failure because of curve fitting difficulties. This causes an inconsistency when the damage curve and residual strength degradation diagrams are drawn with conventional life equations For instance, a value other than static strength is used (q-intercept of S-N curve or fatigue coefficient of Basquin's relation) or life equation does not coincide with the residual strength degradation curve at the starting point [6, 7].

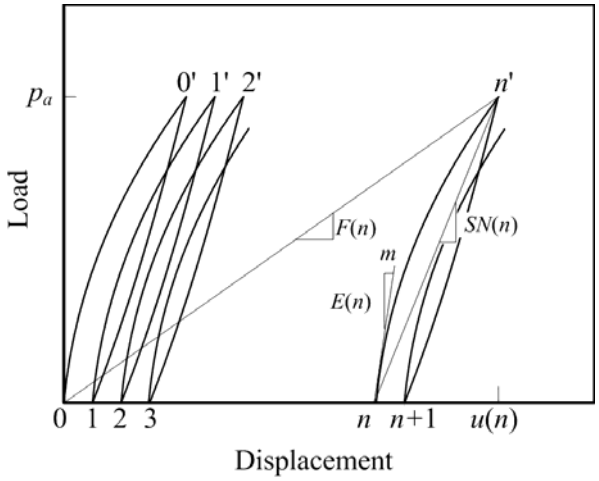

Fig. 4. Fatigue modulus concept.

Hwang's Equation was derived from the concept of the fatigue modulus, which is defined as a function of the loading cycle numbers n, and the applied load level q.

$$F(n,q) = \frac{P_a}{u(n)} = P_u \frac{q}{u(n)} \quad (4)$$

where F is the fatigue modulus, P_a is the applied load, $u(n)$ is the resulting displacement, P_u is the ultimate load, and q is the ratio of the applied load to the ultimate load. This is shown in Fig. 4.

Hwang's equation has the most complicated form of the three equations. The S-N Curve is equivalent to Hwang's Equation when B and C are 1, and yields a straight line in semi-log scale. Basquin's relation gives a straight line in log-log scale. These equations have generality and wide applicability.

5 Experimental Details

The Nano-UTM is designed to measure the mechanical properties of small specimens, with a maximum load of 500 mN and a load resolution of 50 nN.

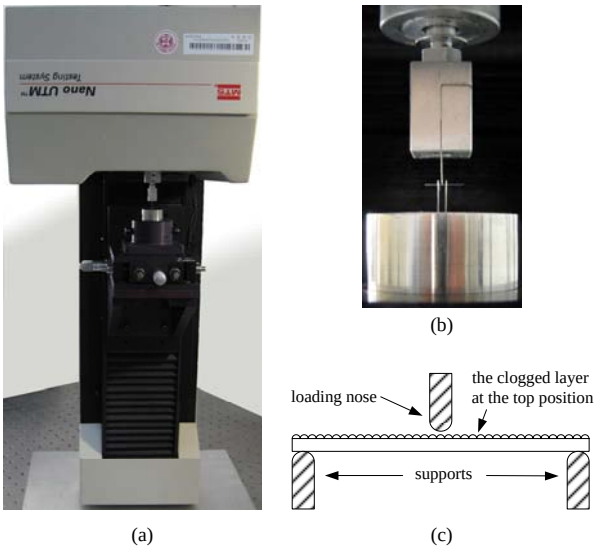

Fig. 5. Bending fatigue testing of the nanohoneycomb. (a) General view. (b) Magnified view. (c) Position of the clogged layer.

Fig. 5a shows the three-point bending configuration of the Nano-UTM, and Fig. 5b shows a magnified view near the specimen. The span length between the lower contact points was 1.09 mm. The width of the specimen was 137 μm and the thickness was 57 μm. The maximum loading distance of the upper fixture was 2 mm. The test was carried out in load-controlled mode. Static bending tests were performed at 0.5 mN/s until failure. The static fracture load when the clogged layer was uppermost was

generally larger than when lowermost. This can be explained from the geometry of the clogged layer and crack propagation under tensile loading. During the bending test, when the clogged layer was lowermost, the clogged layer underwent tensile loading, and the notches on the clogged layer functioned as a crack tip enabling the crack to propagate. When the clogged layer was uppermost, the crack on the notch of the clogged layer did not propagate, because it underwent compressive loading. It appears that these crack tips reduce the fracture strength under tensile load. The fatigue test was carried out with the clogged layer uppermost as is shown Fig. 5c.

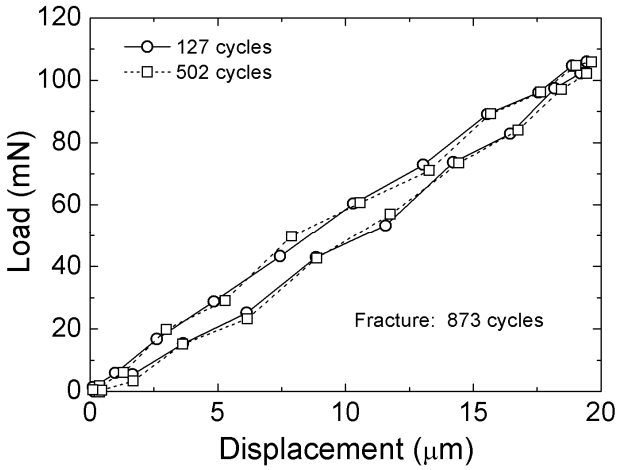

Fig. 6. Cyclic load-displacement behavior at 0.86 of static fracture load.

The fatigue tests were carried out under a load-controlled mode with a sinusoidal waveform applied at a frequency of 0.8 Hz, which should only cause a negligible temperature increase during testing. Applied load levels were determined at normalized values of 0.86, 0.82, 0.78, 0.73, and 0.69 for the static fracture load; the minimum load during cyclic load was set to zero. A small electro-static force was applied between the specimen and the fixture to prevent sliding when the cyclic load was zero. All tests were carried out at constant room temperature and humidity.

6 Result and Discussions

Fourteen samples were subjected to the static bending test. The fracture load was between 109 and 142 mN, with an average value of 123 mN. Fig. 6 shows the resulting displacements for the load levels at 0.86. These results show a very small increase of both resultant and permanent displacement with the number of cycles. This suggests that it is difficult to estimate a fracture cycle by examining resultant displacement during tests. The relation between the resultant displacement and fatigue cycle for some samples is shown in Fig. 7. The increase of the resultant displacement was small. Fig. 8 shows the relation of static fracture strain and fatigue resultant strain. The fatigue fracture stress and strain were normalized to the static fracture values. As load level decreased, the resultant fracture strain decreased. For composite materials and sandwich structures, it is reported that the resultant fracture strain is proportional to the load level [6]. However the nanohoneycomb structure showed different behavior.

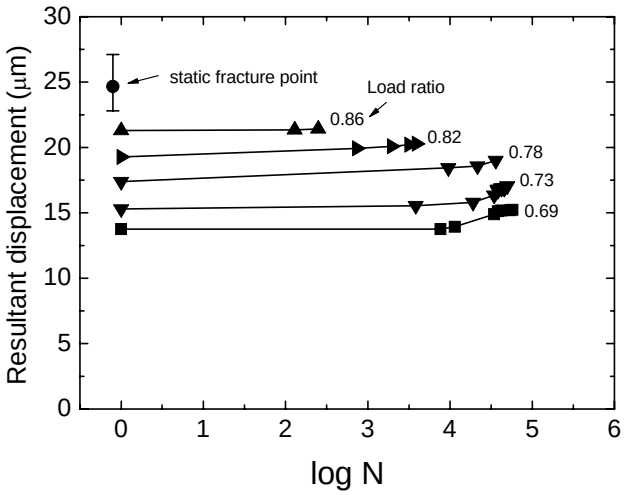

Fig. 7. Resultant displacement versus number of cycles for a sample of experimental results.

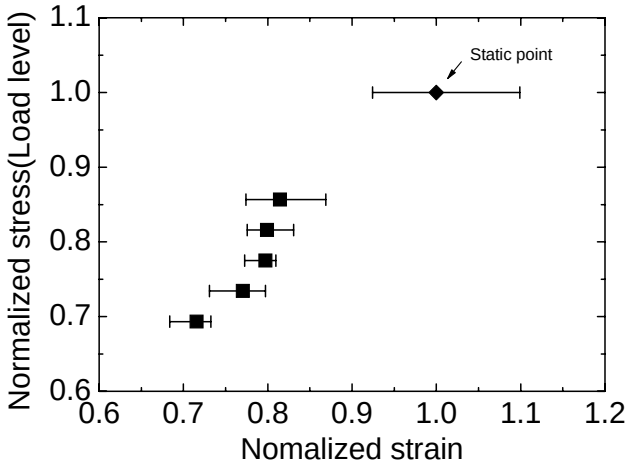

Fig. 8. Relation of static ultimate strain and fatigue resultant strain.

The fatigue test results are summarized in Table 1, and fatigue life data and prediction curves for the mean values of the fatigue cycle are shown in Fig. 9. The results using the arithmetic mean value for the fatigue cycle are as follows [6]:

Hwang's Equation:

$$N = [32100(0.947^{0.00109} - q^{0.00109})]^{1/0.208} \quad (R^2 = 0.98) \tag{5}$$

Basquin's Relation:

$$N = (q/1.089)^{-1/0.0378} \quad (R^2 = 0.95) \tag{6}$$

S-N Curve:

$$q = -0.0675 \log N + 1.041 \quad (R^2 = 0.96) \tag{7}$$

Table 1. Static and fatigue test summary.

Static Test	Fracture load (mN)				No. of samples
	Average	Min.	Max.	Standard deviation	
	123	109	142	13	14
	Effective bending modulus (GPa)				
	Average	Min.	Max.	Standard deviation	
	62.5	57.5	69.4	3.2	

Fatigue Test						
Load level	Load (mN)	Fracture cycle				No. of samples
		Arith. mean	Min	Max	Standard deviation	
0.86	105	393	57	873	348	4
0.82	100	2,839	1,953	4,148	1,157	3
0.78	95	16,538	867	35,905	18,345	4
0.73	90	25,983	2,056	57,402	22,932	5
0.69	85	103,782	6,054	342,279	160,077	4

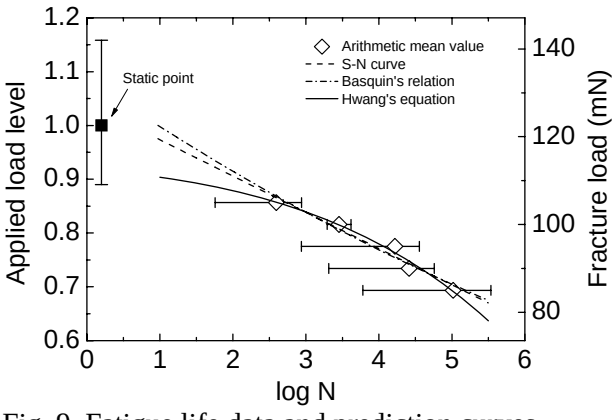

Fig. 9. Fatigue life data and prediction curves.

The mean values and the theoretical curves show good agreement, although there is a wide range of experimental data. It is found that Hwang's equations predicted fatigue life better than the conventional S-N curve or Basquin's relation. This is due to the nonlinearity between the applied load level and the mean logarithm value of the fatigue fracture cycle, as Hwang's equation has more parameters to express this nonlinearity than the other equations. For most specimens the fractured surface showed similar geometry.

7 Conclusions

(i) Nanohoneycomb beam specimens were obtained using a two-step fabrication process. During fabrication each beam-shaped specimen was securely fastened at both ends, and the specimen was extracted by breaking near the ends. This enabled us to obtain a large number of good beam-shaped specimens in a single process.

(ii) The static and fatigue properties of the nanohoneycomb structures were ascertained by a three-point bending test using a Nano-UTM. The mean values of the experimental results and the theoretical curves were in good agreement, although there is a wide range of experimental data.

(iii) The fatigue resultant strain was smaller than the static fatigue strain. It decreased as load level decreased, with a non-linear relation. The increase of resultant strain during the cyclic load was very small. Hence, it seems that it is difficult to estimate the fatigue cycle by observing increases of resultant strain during a fatigue test.

(vi) If tension is applied to the clogged layer, the bending fracture load decreases, because the clogged layer acts as a crack tip. In structural uses of nanohoneycomb, it is preferable that the clogged layer supports compression or is removed.

ACKNOWLEDGEMENTS

This work was supported by Grant No. R01-2006-000-10585-0 (2006) from the Korea Science and Engineering Foundation (KOSEF), to which the authors are grateful.

References

[1] Hynes A. M. et al. "Recent advances in silicon etching for MEMS using the ASE process". *Sensor Actuat. A-Phys.*, Vol. 74, pp. 13-17, 1999.

[2] Gad-el-Hak Mohamed et al. "*The MEMS handbook*," Chap. 17., CRC Press, 2002.

[3] Masuda H. et al. "Ordered metal nanohole arrays made by a two-step replication of honeycomb structures of anodic alumina". *Science*, Vol. 268, pp. 1466-1468, 1995.

[4] Hwang W. et al. “Single- and multi-stress level fatigue life prediction of glass/epoxy composites”. *J. Adv. Mat*., Vol. 26, No. 4, pp. 3-9, 1995.

[5] Kim D. H. et al. “Fatigue Characteristics of Surface Antenna Structure Designed for Satellite Communication”. *J. Reinf. Plast. Compos.*, Vol. 24, No. 1, pp. 35-51, 2005.

[6] Hwang W. et al. “Fatigue of composite-fatigue modulus concept and life prediction”. *J. Compos*., Vol. 20, pp. 154-165, 1986.

[7] Hwang W. et al. “Single- and multi-stress level fatigue life prediction of glass/epoxy composites”. *J. Adv. Mat.*, Vol. 26, No. 4, pp. 3-9, 1995.